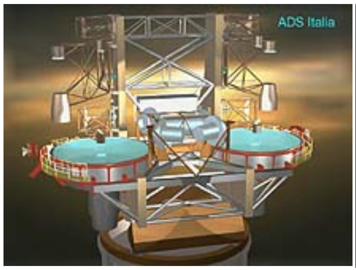




# LBT PROJECT

# 2 × 8.4 m OPTICAL TELESCOPE

# AO Demonstrator Project

# Predicted Imaging Performance

| | Signature | Date |
|---|---|---|
| Prepared | R. F. Green & R. M. Wagner | March 8, 2011 |
| Reviewed | J. Brynnel, D. Thompson, J. Hill | |
| Approved | J. Brynnel | |

# 1. Revision History

| Issue | Date | Changes | Responsible |
|---|---|---|---|
| a | 8-Mar-11 | First draft | RFG and RMW |
| | | | |
| | | | |
| | | | |

## 2. Table Of Contents



## 3. About this document

### 3.1. Purpose

This document describes the expected imaging performance of the LBT AO system combined with the PISCES JHK imaging camera.

## 4. Performance Description for LBT Adaptive Optics Unit#1

The LBT Adaptive Optics system was designed to achieve high performance, reliability, and efficiency. Characterization on sky was carried out with a commercial InGaAs infrared test camera with a thermo-electric cooler. Most of the observations were performed in the H-band; K-band was not available. The fundamental references are Riccardi et al., 2010, SPIE, 7736-82, and Esposito et al., 2010, SPIE, 7736-12.

### 4.1. Reference star magnitude and seeing

Achieved Strehl ratio was measured as a function of reference star magnitude and seeing condition. The ‘R+I’ magnitude plotted is basically a catalogue R magnitude corrected for the wavelength range of the wavefront sensor from 600 to 950 nm. Use of the catalogue R magnitude should predict the recorded counts to within 0.5 mag. Note that the seeing values are mainly from the on-telescope DIMM, which has not yet been fully calibrated. Achieved Strehl Ratio depends on the brightness of the reference star, the observing wavelength, the uncorrected seeing, and the distance from the reference star as are discussed below.

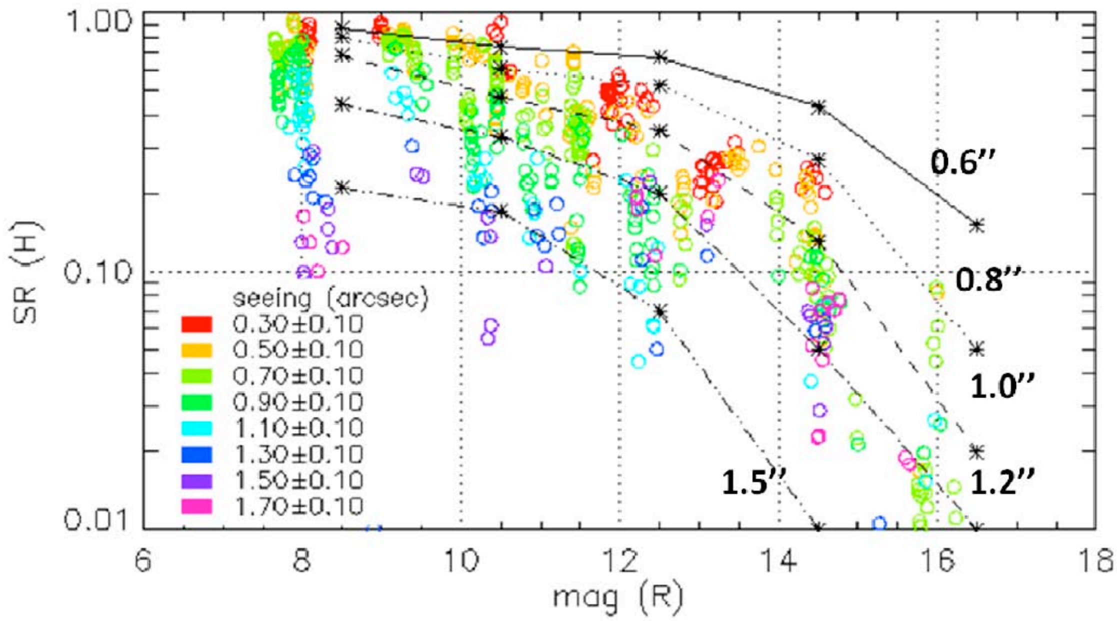


Figure 1 The plot od SR in H band versus star magnitude in R band. The four lines represent results from numerical simulations. Note that the seeing estimate, found from AO diagnostic data, is optimistic for magnitudes value fainter than 12-13.

The plot and image below show the AO-corrected image for a 20-second exposure in the H-band of a star with an R magnitude of 7.2. The achieved Strehl ratio is 86%, with the FWHM of the core measured at the expected value of 40 milli-arcseconds. The maximum contrast of $10^4$ is achieved at 0.4-arcsecond radius, just inside of the turbulence residual halo. The prediction for 500 corrected modes agrees with the peak of that residual occurring at ~0.55 arcsecond.

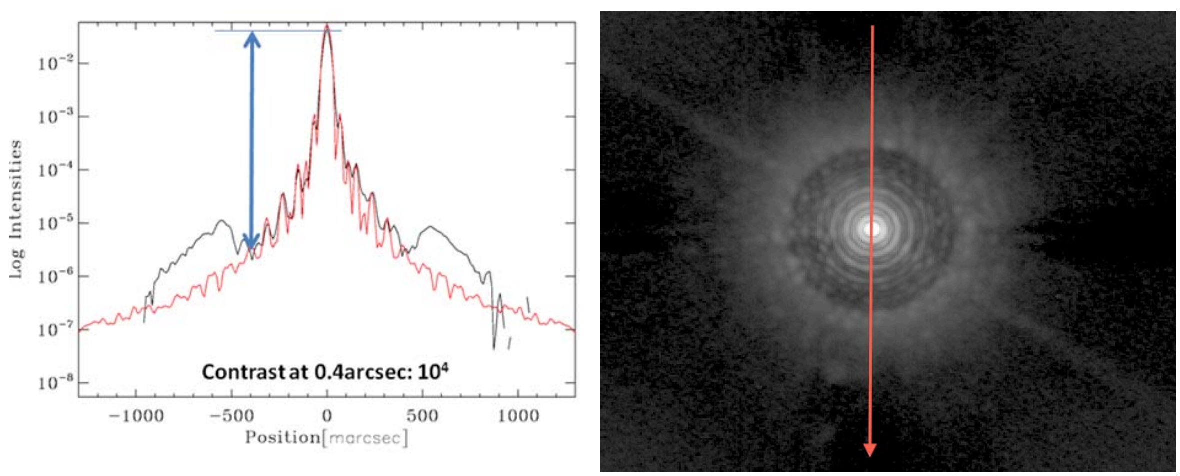


**Figure 2. Comparison between diffraction-limited PSF profile (red line) and AO-corrected PSF (black line) in the H-band. The reported profile section is highlighted in the figure on the right, which has a Strehl ratio exceeding 80%.**

## 4.2. Strehl ratio wavelength dependence

To scale the expected Strehl ratio in the H-band to that anticipated for some other band, the Arcetri team has found success using the Maréchal approximation. That approach is based on the derivation that the *Strehl ratio* $\approx exp(-2\pi\sigma^2)$, where σ is the RMS aberration amplitude as a fraction of the central wavelength of the band. Therefore, it follows that

$$SR(\lambda) = SR(H)^{(\frac{1.65}{\lambda})^2}$$

where SR is the Strehl Ratio, SR(H) is the Strehl Ratio in the H-band, and λ is the central wavelength in microns of the band of interest. For example, the team reports that they achieved 65% Strehl in the H-band on a particular star, and simultaneously measured 20% Strehl in the I-band, consistent with the numerical prediction.

## 4.3. Impact of vibrations

In these earliest days of AO operation at the LBT, there are sometimes uncorrected vibrations, possibly wind-induced. The IR Test Camera allowed the team to take short exposures on bright objects, then either sum them directly or shift and add based on peak position. The uncompensated jitter amounts to 5-10 mas, so that the shift-and-add image showed an improvement of a factor of 1.2 in peak intensity. This effect is most relevant for reference stars fainter than ~$10^{th}$ mag, where the correction bandwidth must be reduced, leaving some uncompensated jitter.

## 4.4. Reference star considerations

Should the reference star be separated in angle from the target to be corrected, the atmospheric turbulence will degrade the quality of the correction as the separation is increased. A reasonable expectation for median seeing, based on the commissioning observations, is an isoplanatic patch in the H and K bands of ~20 arcseconds ($\theta_0$), at the edge of which the degradation in Strehl ratio should be 0.37 according to the following formula. Fried's theory predicts that the quality of the correction will degrade with separation θ as $exp[-(\theta/\theta_0)^{5/3}]$.

## 4.5. Setup and overheads

Experience to date suggests that setup for AO imaging should be relatively efficient. From an evaluation of all presets of LUCI during fall semester 2010, it was found that 77% of active presets completed successfully (meaning the guide star was identified and centered on the hot spot). That value is a lower limit for on-sky performance, given that it includes some test operations that were expected to fail. The median time for presetting to a new field was 52 seconds, with the maximum time 227 seconds (the latter probably including an azimuth unwrap). The failures to acquire the guide star were from a number of causes: guide star out of probe range, guide star coordinate or magnitude errors, guide star peak dimming from clouds or poor seeing, or telescope pointing errors. The latter was a significant contributor, but is being actively worked on with a collimation + pointing model approach that has been demonstrated to be more robust with sky position and temperature.

The controls approach is that the peripheral wavefront sensor conditions the active optics through sufficient cycles to bring the wavefront error below a fixed value. Each cycle takes about 45 seconds (limited by a long enough integration to average over low-order atmospheric wavefront disturbances and by the primary mirror actuators to settle to within tight tolerance). Convergence in three cycles is a typical outcome for the rigid secondary. Early performance with the AO secondary required 4 cycles; improvements underway are anticipated to reduce that value to three or possibly better.

Once the active optics have converged, the AO system takes control of wavefront corrections, with the AO wavefront sensor interacting directly with the adaptive secondary mirror. Using input information about seeing and reference star brightness, the AO system chooses the WFS sampling frequency and the number of modes to correct, then runs an optimization routine to fine tune the low- and high-order gains. The entire automatic process takes less than 5 minutes from internal handover to the AO wavefront sensor until optimized lock.

The expectation for overheads is therefore less than 10 minutes to change AO imaging fields, with accurately supplied field and guide coordinates and stable conditions. Dither-type offsets can be done by pausing the AO loop, repositioning the telescope, reacquiring the reference star, and resuming AO correction. This AO reacquisition is a modest increment on the total time to offset; LUCI offsets in seeing-limited mode take a median time of ~14 seconds. Offsetting in AO mode should take well under 1 minute.

Under stable conditions, the AO system holds lock for more than an hour at a time, so imaging exposures with narrow-band filters should pose no fundamental difficulty. The typical commissioning test exposure sequence was 6 × 15 seconds, but some "astronomical" exposures were taken in the range of 5-10 minutes total accumulation. Beyond the effect of vibration noted above, there were no operational issues with the AO system on the longer exposures.

# 5. Science Instrument and Camera

## 5.1. Description

Among several choices of possible science cameras and instruments that could exploit the benefits and capabilities of the LBT AO system, we have chosen to utilize the PISCES infrared camera (Fig. 3) used by the University of Arizona. PISCES is a PI instrument designed and built by Dr. Don McCarthy of Steward Observatory, students, and collaborators. PISCES utilizes a HAWAII-1 1k × 1k HgCdTe pixel, 1 – 2.5 μm detector.

The optical design uses six lenses with spherical surfaces which all are cooled to 77 K by liquid nitrogen. The design also incorporates accurate pupil reimaging and cold baffling to block thermally emissive telescope structures. A single 10-position manually operated filter wheel provides a broad selection of broad and intermediate band filters and grisms. Interested users can find additional details in the description of the instrument provided by McCarthy et al. (2001, PASP, 113, 353-361).

At the LBT, the f/15 Gregorian beam is reimaged in the instrument to a focal ratio of f/22 providing a field of view of about 21 arcsec in diameter at a pixel scale of 0.022 arcsec/pixel. When used at the LBT, PISCES under-samples the core in J, critically samples it in H, and over-samples it in K. We are currently investigating implementing remote control of the manual filter wheel. In addition, the filter wheel uses 1-inch (25.4 mm) diameter filters so the opportunity may exist to use specialized filters for AO science programs.

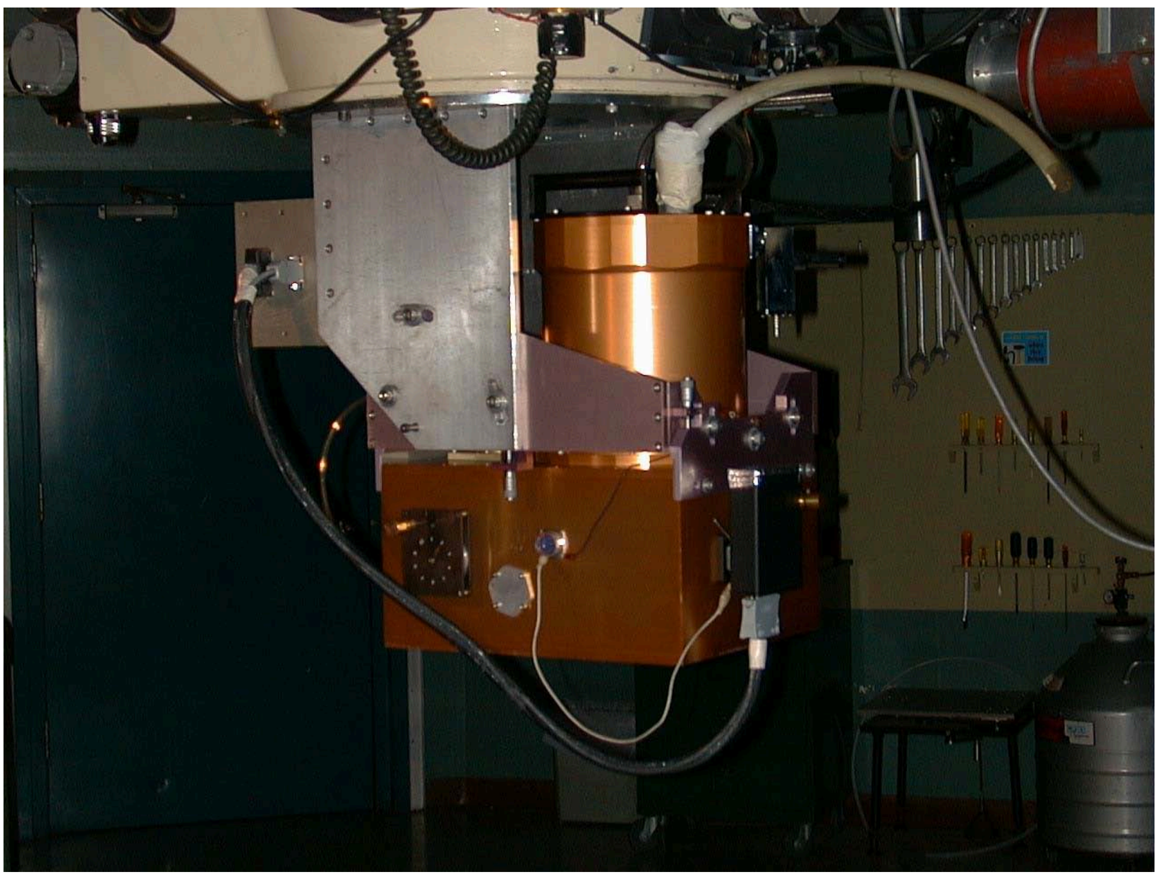

**Figure 3. The PISCES infrared camera attached to the Steward Observatory Bok 2.3 m telescope.**

### 5.2. General specifications

In Table 1, we summarize the general specifications of PISCES and its use on the LBT.

**Table 1. General specifications of the PISCES infrared camera and detector.**

| | |
|---|---|
| Input f/ ratio | f/15; reimaging to f/22 |
| Wavelength range | 1 – 2.5 μm |
| Field of view | ~21 arcsec ∅ |
| Pixel scale | 0.022 arcsec/pixel |
| Filters | Currently installed: J, H, Ks, J-continuum, open, dark, 2.140 μm, 2.086 μm, Fe II (1.64 μm), 1.083 μm |
| Detector | Hawaii-1 (HgCdTe) array, 1k × 1k pixel format, 18 μm pixels, QE is typically 60% in JHK |
| Gain | 4.4 $e^-$/ADU |
| Read noise | ~20 $e^-$ (for double-correlated sampling) |
| Dark current | Unknown |
| Linearity | Linear range is <90 $ke^-$ |
| Readout modes | Double-correlated and Fowler sampling, minimum readout, 0.8 sec (3μs pixel clock), frames can be co-added, rapid readout (2-30 Hz) of smaller regions of interest (subarray mode) |

### 5.1. Sensitivity

The performance of PISCES on the 2.3 m telescope is summarized by McCarthy et al. (2001) in their Figure 2. They find limiting magnitudes (10σ) in J, H, and Ks of 18.2, 17.3, and 16.3 respectively in 60 seconds. We have used these measurements to estimate the expected AO performance of PISCES on the LBT.

The results are presented in Fig. 4 where we show the S/N ratio in 1 hour for a point source as a function of the effective K-band magnitude. We assume a sky brightness of 13 mag/arcsec$^2$ in the example. Two curves are shown. The upper curve corresponds to an aperture of 1.0*FWHM while the lower curve corresponds to an aperture of 2.0*FWHM. In both cases, the results shown assume a Strehl Ratio of 1.0.

We predict that PISCES on LBT/AO will achieve a limiting K-band magnitude (10σ) of 22.4-23.2 magnitude in 1 hour. The results compare favorably with other IR instruments operating on large telescopes. We find that NIRC2 in NGS AO-mode on Keck achieves a limiting K magnitude of 23.7 in 1 hour (10σ) while we estimate that LUCIFER may achieve a limiting K magnitude of 23.6 in 1 hour (10σ). In fact, the NIRC2 exposure time calculator gives a reasonable performance estimate including Strehl Ratio when the difference in collecting area between the two telescopes is taken into account.

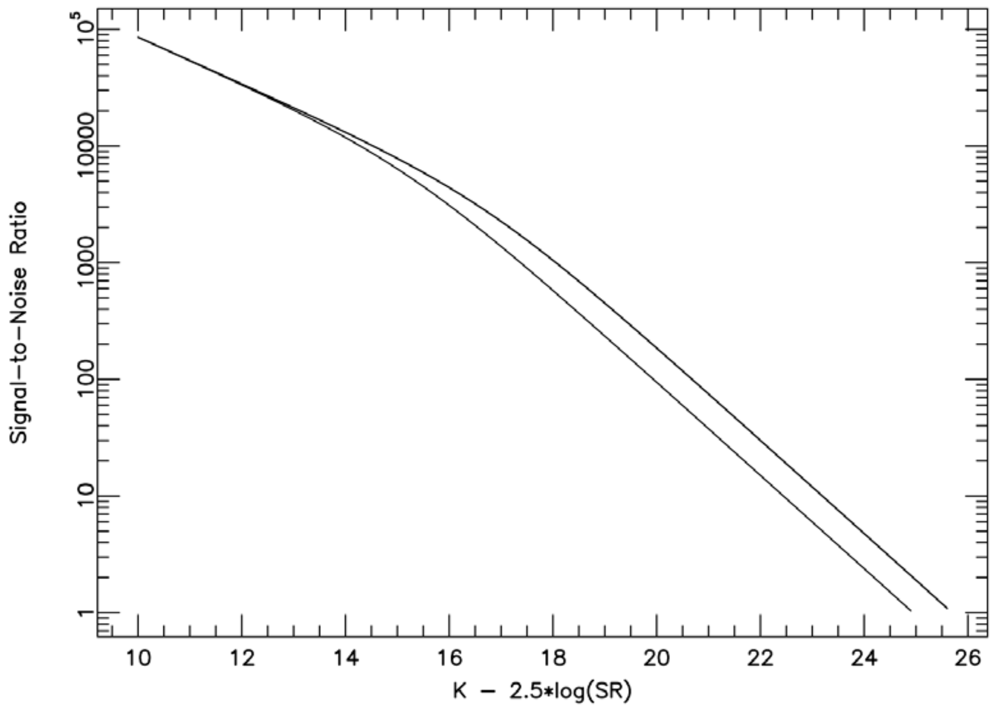


**Figure 4. Signal-to-noise ratio in 1 hour as a function of the effective K-band magnitude. The upper curve corresponds to an aperture of 1.0*FWHM while the lower curve corresponds to the performance assuming an aperture of 2.0*FWHM. Both curves assume a Strehl Ratio of 1.0. A sky brightness of 13.0 mag/arcsec$^2$ is assumed.**

**--oOo--**